A Nonlinear Differential Semblance Strategy for Waveform Inversion: Experiments in Layered Media

Dong Sun and William W Symes, Rice University*

SUMMARY

This paper proposes an alternative approach to the output least-squares (OLS) seismic inversion for layered-media. The latter cannot guarantee a reliable solution for either synthetic or field data, because of the existence of many spurious local minima of the objective function for typical data, which lack low-frequency energy. To recover the low-frequency lacuna of typical data, we formulate waveform inversion as a differential semblance optimization (DSO) problem with artificial low-frequency data as control variables. This version of differential semblance with nonlinear modeling properly accounts for nonlinear effects of wave propagation, such as multiple reflections. Numerical experiments with synthetic data indicate the smoothness and convexity of the proposed objective function. These results suggest that gradient-related algorithms may successfully approximate a global minimizer from a crude initial guess for typical band-limited data.

INTRODUCTION

The full waveform, output least squares (OLS) inversion is the most common model-based data-fitting approach to the inverse problem in reflection seismology of inferring subsurface properties from shallow-seismic data. OLS inversion is conceptual attractive because: (1) its objective is very simple and expresses the maximum likelihood criterion, given that experimental errors have Gaussian distributions; (2) it does not require picked travel time and can take into account essentially any physics of seismic wave propagation and reconstruct detailed features of subsurface structure.

However, the direct application of OLS inversion in relection seismology has been strictly limited. The principle impediment to this approach is well discussed in literature, (Gauthier et al., 1986; Santosa and Symes, 1989; Tarantola et al., 1990; Symes and Carazzone, 1991; Bunks et al., 1995; Shin and Min, 2006, just to name a few). Because its objective is very ill-conditioned and possesses lots of spurious local minima, OLS inversion doesn't work with any descent method (mandatory because of problem size) unless the initial model has the long scale structure of the true model.

The main factor accounting for the above behavior of OLS inversion is the band-limitation of typical field data, especially the lack of low frequencies. Low-frequency data appear to contain information about the trend of the true model. OLS inversion cannot infer the model trend from bandlimited reflection data. Lots of work has shown that the impedance as a function of vertical travel time in a layered acoustic medium could be reconstructed from the impulse response, which contains all frequency components down to 0 Hz, (Bamberger et al., 1979; Bube and Burridge, 1983; Symes, 1986; Sacks and Santosa, 1987). For several dimensional problem, numerical examples indicate that impulse responses may determine constant-density acoustic models via OLS inversion (Bunks et al., 1995; Shin and Min, 2006).

With the above observation on the solvability of the impulsive inverse problem, the thesis of this paper is to introduce a differential semblance strategy with nonlinear modeling for waveform inversion to recover the missing low-frequency components in the data and avoid the intrinsic difficulties of OLS inversion. Differential semblance criterion with Born modeling has been discussed in detail in (Symes and Carazzone, 1991; Symes, 1993, 1999; Chauris and Noble, 2001; Mulder and ten Kroode, 2002; Shen et al., 2003, 2005; de Hoop et al., 2005; Albertin et al., 2006; Shen and Symes, 2008). The underlying idea is the concept of semblance of redundant images, i.e., due to the high redundancy of a typical survey, predictions of some model parameters are redundant and unlikely to be consistent (flat in common image panels) unless the velocity model is correct. This paper presents a nonlinear version of differential semblance to properly account for nonlinear effects of wave propagation.

As the first step of developing such an algorithm, this paper discusses a simple model for reflection seismology — the layered constant-density acoustic model. The next two sections decribe this nonlinear differential semblance approach and demonstrate the smoothness and convexity of its objective via numerical experiments. Finally, the paper ends with a description of some refinements of this approach.

THEORY AND METHOD

Problem Setting

In the layered constant-density acoustic model, the wave field potential $u(x,z,t)$ ($x,z \in I\!R$) is governed by the wave equation

$$\begin{aligned} \left(\frac{1}{c^2(z)}\frac{\partial^2}{\partial t^2} - \nabla^2\right) u(x,z,t) &= w_b(t)\delta(x,z), \\ u(x,z,t) = u_t(x,z,t) &\equiv 0, \qquad t<0, \end{aligned} \tag{1}$$

where $c(z)$ is the acoustic velocity field depending only on the depth z, and the right-hand side is an isotropic point energy source with the source wavelet $w_b(t)$. Notice that $w_b(t)$ is usually chosen to be band-limited, as is required by observations of the spectra of seismograms: for various physical limitations, real reflection seismograms don't have fourier components at very low ($< \omega_l$ Hz) and very high ($> \omega_h$ Hz) temporal frequencies [*].

Regarding the source (i.e., $w_b(t)$) as known, the pressure field, hence the seismogram, becomes a function of the acoustic velocity:

$$s[c](x,t) := \frac{\partial u}{\partial t}(x,0,t), \;\; 0 \le t \le t_{max}.$$

[*]The positive numbers ω_l and ω_h depend on specific physical settings of real experiments. For example, $\omega_l = 5, \omega_h = 60$.

The goal is to find $c(z)$ for $0 \le z \le z_{max}$ from the observed seismogram s_{data} such that $s[c] \simeq s_{data}$.

The first step of constructing the proposed approach is the introduction of the Radon transformed field

$$U(z,p,t) = \int dx\, u(x,z,t+px), \quad p \in I\!R.$$

A staightforward calculation shows that the original problem becomes a set of 1-D plane-wave problems

$$\begin{aligned} \left(\frac{1}{v^2(z,p)}\frac{\partial^2}{\partial t^2} - \frac{\partial^2}{\partial z^2}\right) U(z,p,t) &= w_b(t)\delta(z), \\ U(z,p,t) = U_t(z,p,t) &\equiv 0, \qquad t<0, \end{aligned} \tag{2}$$

for suitably small $p \ge 0$ so that $c\,p < 1$, where the *vertical velocity*

$$v(z,p) := c(z) \Big/ \sqrt{1-c^2(z)p^2}\,, \quad \texttt{for } p < p_{max} = 1/c_{max}\,,$$

and p denotes the ray parameter (slowness).
The plane-wave seismogram is then defined as

$$\begin{aligned} &F_{w_b}[c](p,t) := \frac{\partial U}{\partial t}(p,0,t) \\ &\texttt{for } (p,t) \in \mathbf{P} := \{(p,t) : |p| \le p_{max}, 0 \le t \le t_{max}\}\,, \end{aligned} \tag{3}$$

which presents a forward map $F_{w_b} : \mathbf{M} \longrightarrow \mathbf{D}$, where $\mathbf{D}$ is the *data space*, and the *model space* $\mathbf{M}$ denotes a set of possible velocity models, incorporating bounds on values and other regularity constraints.

Given the plane-wave seismogram $d \in \mathbf{D}$ (i.e., $d = S_{data}$ [†]), this paper focuses on the inverse problem:

$$\begin{aligned} \texttt{Find} \quad & c(z) \in \mathbf{M} \\ \texttt{such that} \quad & F_{w_b}[c] \simeq d. \end{aligned} \tag{4}$$

To explain the construction of the proposed approach, we will first rewrite the inverse problem (4) via a unifying concept —— Extended Modeling, introduced in (Symes, 2008) to build a general framework for the inverse problem of reflection seismology.

Extended Modeling

Take for the extended model space $\overline{\mathbf{M}}$ a set of positive functions $\bar{c}(z,p)$ of depth z and slowness p. The extension map E simply views a physical velocity $c(z)$ (positive function of z) as a function of z and p, i.e. as constant in p: $E[c](z,p) := c(z)$. Then, the corresponding vertical velocity to $\bar{c}(z,p)$ is

$$v(z,p) := \bar{c}(z,p) \Big/ \sqrt{1-\bar{c}^2(z,p)\,p^2}\,,$$

and the extended forward map $\overline{F}_{w_b} : \overline{\mathbf{M}} \longrightarrow \mathbf{D}$ is defined as

$$\overline{F}_{w_b}[\bar{c}](p,t) := \frac{\partial U}{\partial t}(p,0,t) \qquad \texttt{for all } (p,t) \in \mathbf{P}, \tag{5}$$

where $U(z,p,t)$ satisfies (2) with c replaced by $\bar{c}$. Hence, the extended modeling operator $\overline{F}_{w_b}$ satisfies the prerequisite: $F_{w_b}[c] = \overline{F}_{w_b}[E[c]]$ for any $c \in \mathbf{M}$.

[†] S_{data} can be computed from s_{data} by Radon Radon transform. To focus on the principal algorithm, we leave out computation and assume that S_{data} is known.

Notice that the extension map E is one-to-one, hence enable one to view the model space $\mathbf{M}$ as a subset of the extended model space, i.e., $E[\mathbf{M}] \subset \overline{\mathbf{M}}$. Since the extended models will be "unphysical" in the sense that $\bar{c}(z,p) \in \overline{\mathbf{M}}$ could vary in p, $E[\mathbf{M}]$ consists of the "physical models".

The extended inverse problem becomes:

$$\texttt{given } d \in \mathbf{D}, \ \texttt{find } \bar{c}(z,p) \in \overline{\mathbf{M}} \ \texttt{such that } \overline{F}_{w_b}[\bar{c}] \simeq d.$$

A solution $\bar{c}$ is physically meaningful only if $\bar{c} = E[c]$ for some $c \in \mathbf{M}$. In that case c becomes a solution of the original inverse problem (4), i.e. $F_{w_b}[c] = \overline{F}_{w_b}[\bar{c}] \simeq d$. That is, *solving the inverse problem* (4) *is equivalent to find a solution to the extended inverse problem that belongs to* $E[\mathbf{M}]$. (Generally, "$\simeq$" is in the least-squares sense.)

To turn this inversion into an optimization procedure, one needs an objective to measure the extent to which a solution to the extended inverse problem is physically meaningful. Here, we choose the linear map $A[\bar{c}] := \frac{\partial \bar{c}}{\partial p}$, which satisfies the equivalence condition :

$$\bar{c} \in E[\mathbf{M}] \Longleftrightarrow A[\bar{c}] = 0 \quad (\texttt{coherency condition}). \tag{6}$$

With the above notations, a differential semblance form of the inverse problem is:

$$\begin{aligned} \min_{\bar{c} \in \overline{\mathbf{M}}} \quad & J_A[\bar{c},d] := \frac{1}{2}\,\|A[\bar{c}]\|^2 \\ \texttt{such that} \quad & \left\|\overline{F}_{w_b} - d\right\|^2_{\mathbf{D}} \simeq 0. \end{aligned} \tag{7}$$

Here, the major issue arise in formulating any approach to the solution of problem (7): *how to parametrize the feasible set* $\mathscr{F} = \left\{\bar{c} \in \overline{\mathbf{M}} : \left\|\overline{F}_{w_b} - d\right\|^2_{\mathbf{D}} \simeq 0\right\}$*?*

An answer to this question comes from the solvability of the impulsive inverse problem. Next we will extract the relation between low-frequency data components and extended velocity models, and build the DS approach based on this relation.

Differential Semblance Approach

Recall that problem (1) is reduced to a set of 1D plane-wave problems (2) via Radon Transform. The solvability of 1D impulsive inverse problems tells us that with the very-low frequency information, a 1D OLS problem is solvable, i.e. the inversion could recover the long-scale structure.

For each fixed slowness p, given the source time function

$$w_b(t) = \int_{\omega_l < |\omega| \le \omega_h} d\omega\, e^{2\pi i \omega t} g(\omega)$$

and the corresponding reflection response

$$d_b(p,t) = \int_{\omega_l < |\omega| \le \omega_h} d\omega\, e^{2\pi i \omega t}\, \eta(p,\omega),$$

take

$$w(t) = w_l(t) + w_b(t),$$

where

$$w_l(t) = \int_{|\omega| \le \omega_l} d\omega\, e^{2\pi i \omega t} g(\omega).$$

One can associate a vertical velocity $v(z,p)$ for each p with $d(p,t)$ via the 1-D OLS inversion, where

$$d(p,t) = d_b(p,t) + d_l(p,t)$$

and

$$d_l(p,t) = \int_{|\omega|\le\omega_l} d\omega\, e^{2\pi i\omega t}\,\eta(p,\omega).$$

Then, $\bar{c}(z,p)$ is computed through $\bar{c} = v \Big/ \sqrt{1+v^2p^2}$.

As a summary, fixing the source wavelet $w(t)$ with low-frequency components down to 0 Hz and band-limited data $d_b(p,t)$, the extended velocity $\bar{c}(z,p)$ becomes a function of the very low-frequency data $d_l(p,t)$ (or $\eta(p,\omega)$ for $|\omega| \le \omega_l$).

We can now state the DS problem as:

$$\begin{aligned} &\min_{\substack{\eta(p,\omega)\\(p,\omega)\in\Omega}} \quad J_{DS} := \frac{1}{2}\|A[\bar{c}]\|^2 \\ &\texttt{such that} \quad \left\|\overline{F}_w[\bar{c}](p,t) - d_b(p,t) - d_l[\eta](p,t)\right\|_{\mathbf{D}} \simeq 0, \\ &p\in[0,p_{max}] \end{aligned} \tag{8}$$

where $A[\bar{c}] := \frac{\partial\bar{c}}{\partial p}$, $\Omega := \{(p,\omega) : 0 \le p \le p_{max}, |\omega| \le \omega_l\}$.

Actually, J_{DS} is continuously differentiable with respect to η. A straightforward derivation leads to an gradient expression for the DS objective:

$$\nabla J_{DS} = \Pi\, D\overline{F}_w[\bar{c}]\left(D\overline{F}_w[\bar{c}]^T D\overline{F}_w[\bar{c}]\right)^{\dagger} \frac{\partial^2\bar{c}}{\partial p^2},$$

where Π is a projector from data space onto low-frequency data controls, $D\overline{F}_w$ is Born extended modeling and $D\overline{F}_w^T$ is its adjoint, computed by the adjoint state method. The proposed procedure is summarized as:

`Nonlinear DS Algorithm:`
`Initialization:` set c^0, d_l^0, $w(t)$, ε, etc.
`For` $k = 0,1,2,\ldots$

1. Compute the sub-OLS problems for $\bar{c}[d_l^k]$;
2. Compute $J_{DS}^k = \frac{1}{2}\left\|\frac{\partial\bar{c}[d_l^k]}{\partial p}\right\|^2$. If $J_{DS}^k \le \varepsilon J_{DS}^0$, stop; else, continue;
3. Compute $\nabla J_{DS}[d_l^k]$. If $\left\|\nabla J_{DS}[d_l^k]\right\| \le \varepsilon\left\|\nabla J_{DS}[d_l^0]\right\|$, stop; else, continue;
4. Compute d_l^{k+1} via some descent method.

Please refer to (Sun, 2008) for more details of this approach.

NUMERICAL EXPERIMENTS

In this section, we present some primary numerical experiments ("scan" tests) for a four-layer model (Figure 1(a)) with the fixed impulsive source time function (plotted in frequency domain in Figure 1(b)). These tests illustrate the smoothness and convexity of the DS function, as well as some issues in its construction which are the subject of ongoing research. The task is to evaluate the proposed DS objective along line segments in the space of low-frequency controls, i.e., compute the DS objective function at a series of data points D_μ(`for some` $\mu \in [0,1.5]$) defined by

$$D_\mu = \{(1-\mu)D_{lpert}(p_i) + \mu D_{obv}(p_i)\}_{i=1}^{N_p}, \tag{9}$$

where data $D_{lpert}(p_i)$ at slowness p_i ($i = 1,2,\cdots,N_p$) differ from the observed data $D_{obv}(p_i)$ only by their low-frequency components. The low-frequency components (0 to $5Hz$) of D_{lpert} are the corresponding low-frequency components of the seismogram derived from the homogeneous velocity model $c_{hom}(z) = 2$.

Choose $N_p = 50$ and discretize the slowness field p in the way that p^2 is sampled evenly.

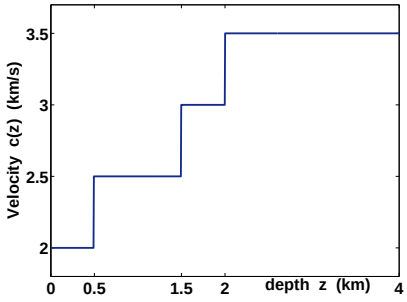

(a)

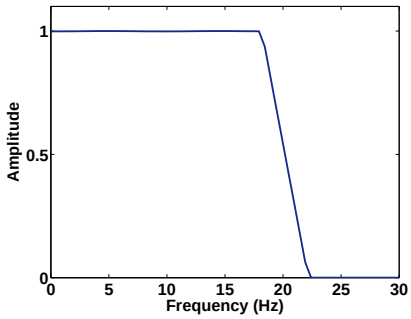

(b)

Figure 1: (a) Four-layer velocity model; (b) Normalized source wavelet in frequency domain (frequency 0 to 25 Hz)).

Experiments with absorbing boundaries

To evaluate the DS objective at a data point, we solve at each slowness the corresponding 1-D least squares problem for $v(z,p)$, then compute $\bar{c}(z,p)$ from $\bar{c} = v \Big/ \sqrt{1+v^2p^2}$, and finally compute the DS objective $J_{DS} = \frac{1}{2}\left\|\frac{\partial\bar{c}}{\partial p}\right\|^2$.

The curve in Figure 2(a) interpolates samples of the DS objective at data points D_μ defined by (9) with $\mu = 0, 0.1, \cdots, 1.5$. This 1-D slice through the DS objective exhibits the smoothness (at least at the sample scale) and convexity. Also, the minimum is achieved at the data point with correct low-frequency components ($\mu = 1$).

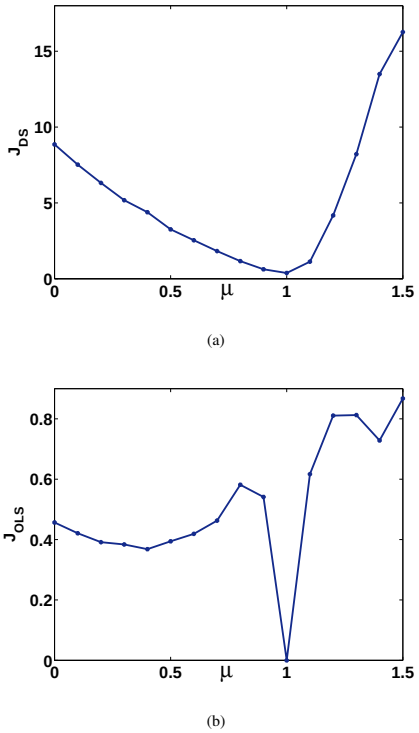

(a)

(b)

Figure 2: With absorbing surface: (a) 1-D scan through the DS objective; (b) 1-D scan through OLS objective

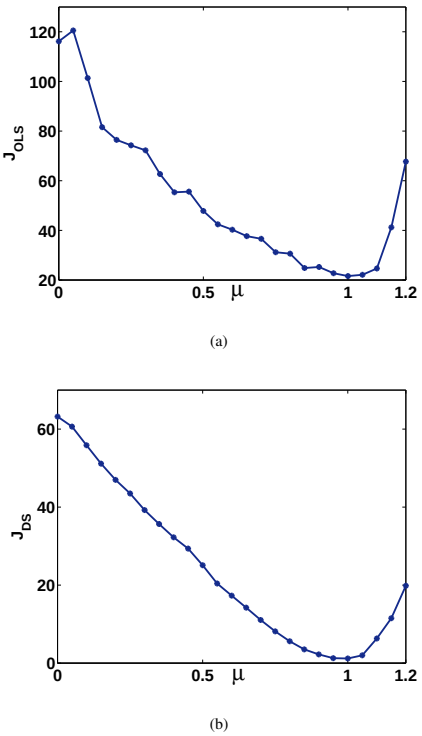

(a)

(b)

Figure 3: With free surface: (a) 1-D scan through the DS objective without postprocessing; (b) 1-D scan through the DS objective with $\bar{c}(z,p)$ smoothed in p

As a contrast, Figure 2(b) presents a similar "scan" experiment, which evaluates OLS objective function at velocity models c_μ chosen as

$$c_\mu(z) = (1-\mu)c_{hom} + \mu c^*(z)$$

with $\mu = 0.0, 0.1, \cdots, 1.5$. This 1-D scan clearly demonstrates the multimodality of OLS objective, which badly jeopardizes the application of gradient-related methods.

Experiments with free surface

An important objective of the proposed algorithm is to account for nonlinear effects of wave propagation such as multiple reflections. Hence, it is desired to know how this DS objective behaves for problems with free surface, which is an important cause of multiple reflections. In the following test, the free surface boundary condition is adopted.

The curves in Figure 3(a) samples the DS objective at data points D_μ with $\mu = 0.0, 0.05, \cdots, 1.2$. Though this scan exhibits the convexity near the minimum, it appears to be flat near $\mu = 1$ and possess some bumps. This adverse behavior may come from the numerical errors accumulated during all the approximating computations. Especially, since the 1D OLS inversions are done independently and yield different accuracy, the extended models $\bar{c}(z,p)$ become inconsistent in slowness, which leads to the noisy behavior of the DS objective.

To improve the behavior of the DS objective, one can adopt a number of strategies to reduce numerical errors, such as using smaller tolerance for 1-D inversions, choosing different expressions of DS objective, and employing some regularization techniques to smooth $\bar{c}(z,p)$ in p and z, etc.. We have considered some of these strategies. Figure 3(b) presents the same scan of the DS objective except that $\bar{c}(z,p)$ is smoothed in p via minimizing the Total Variation of $\bar{c}(z,p)$ with respect to p at each z. Now, the scan exhibits the desired smoothness and convexity.

CONCLUSIONS

This paper presents a nonlinear differential semblance optimization approach to waveform inversion. Numerical examples show that this objective is convex and achieves an extremum at the target model. Thus, gradient-related methods seem promising to solve the proposed DSO problem. Additional techniques need to be implemented to reduce the inconsistency of extended models in slowness. Currently, we reformulate the DSO problem by replacing the 1D OLS subproblems with one 2D least-squares form with a differential semblance type of constraint to penalize the inconsistency in slowness. The new formulation makes this algorithm more generalizable and will lead to better numerical performance. Its implementation is ongoing.

ACKNOWLEDGMENTS

The work reported here was supported by the sponsors of The Rice Inversion Project.

EDITED REFERENCES

Note: This reference list is a copy-edited version of the reference list submitted by the author. Reference lists for the 2009 SEG Technical Program Expanded Abstracts have been copy edited so that references provided with the online metadata for each paper will achieve a high degree of linking to cited sources that appear on the Web.

REFERENCES

Albertin, U., P. Sava, J. Etgen, and M. Maharramov, 2006, Adjoint wave equation velocity analysis: 76th Annual International Meeting, SEG, Expanded Abstracts, TOM 2.1.

Bamberger, A., G. Chavent, and P. Lailly, 1979, About the stability of the inverse problem in 1-d wave equation — Application to the interpretation of seismic profiles: Applied Mathematics and Optimization, **5**, 1–47.

Bube, K. and R. Burridge, 1983, The one dimensional inverse problem of reflection seismology: SIAM Review, 25, 497–559.

Bunks, C., F. Saleck, S. Zaleski, and G. Chavent, 1995, Multiscale seismic waveform inversion: Geophysics, **60**, 1457–1473.

Chauris, H., and M. Noble, 2001, Two-dimensional velocity macro model estimation from seismic reflection data by local differential semblance optimization: Applications synthetic and real data sets: Geophysical Journal International, **144**, 14–26.

de Hoop, M., S.-K. Foss, and B. Ursin, 2005, Depth-consistent reflection tomography using PP and PS seismic data: Geophysics, **70**, no. 5, U51–U65.

Gauthier, O., A. Tarantola, and J. Virieux, 1986, Two-dimensional nonlinear inversion of seismic waveforms: Geophysics, **51**, 1387–1403.

Mulder, W. and A. ten Kroode, 2002, Automatic velocity analysis by differential semblance optimization: Geophysics, **67**, 1184–1191.

Sacks, P. and F. Santosa, 1987, A simple computational scheme for determining the sound speed of an acoustic medium from its surface impulse response: SIAM Journal on Scientific and Statistical Computing, **8**, 501–520.

Santosa, F., and W. W. Symes, 1989, An analysis of least-squares velocity inversion: Geophysical Monograph Series, no. 4, SEG.

Shen, P., and W. Symes, 2008, Automatic velocity analysis via shot profile migration: Geophysics, **73**, no. 5, VE49–VE60.

Shen, P., W. Symes, S. Morton, and H. Calandra, 2005, Differential semblance velocity analysis via shot profile migration: 75th Annual International Meeting, Expanded Abstracts, SEG, 2249–2252.

Shen, P., W. Symes, and C. Stolk, 2003, Differential semblance velocity analysis by wave-equation migration: 73rd Annual International Meeting, SEG, Expanded Abstracts, 2135–2139.

Shin, C. and D. -J. Min, 2006, Waveform inversion using a logarithmic wavefield: Geophysics, **71**, no. 3, R31–R42.

Sun, D., 2008, A nonlinear differential semblance algorithm for plane waves in layered media: Technical Report 09-04, Department of Computational and Applied Mathematics, Rice University.

Symes, W. W., 1986, On the relation between coefficient and boundary values for solutions of webster's horn equation: SIAM Journal on Mathematical Analysis, **17**, 1400–1420.

Symes, W. W., 1993, A differential semblance criterion for inversion of multioffset seismic reflection data: Journal of Geophical Research, **98**, 2061–2073.

Symes, W. W., 1999, All stationary points of differential semblance are asymptotic global minimizers: layered acoustics: Technical Report 99-29, Department of Computational and Applied Mathematics, Rice University.

Symes, W. W., 2008, Migration velocity analysis and waveform inversion: Geophysical Prospecting, **56**, 765–790.

Symes, W. W., and J. Carazzone, 1991, Velocity inversion by differential semblance optimization: Geophysics, **56**, 654–663.

Tarantola, A., E. Crase, M. Jervis, Z. Konen, J. Lindgren, K. Mosegard, and M. Noble, 1990, Nonlinear inversion of seismograms: State of the art: 60th Annual International Meeting, SEG, Expanded Abstracts, 1193–1198.